Chapter 11
Central Carbon Metabolism and Respiration in *Gluconobacter oxydans*

Stephanie Bringer and Michael Bott

Abstract *Gluconobacter oxydans*, an α-proteobacterial species used for industrial vitamin C production, possesses a number of unusual metabolic features. Because of the absence of phosphofructokinase, succinyl-CoA synthetase, and succinate dehydrogenase, the Embden–Meyerhof–Parnas pathway (EMP) and the tricarboxylic acid (TCA) cycle are interrupted, leaving the pentose phosphate pathway (PPP) and the Entner–Doudoroff pathway (EDP) as the only complete pathways in central metabolism. Mutant and ^{13}C-based carbon flux analysis revealed the PPP to be of prime importance for the cytoplasmic catabolism of sugars and derivatives. Pyruvate is partially converted to the end product acetate by pyruvate decarboxylase and acetaldehyde dehydrogenase. The respiratory chain involves two terminal ubiquinol oxidases, cytochrome bo_3 and a cyanide-insensitive *bd*-type oxidase CIO. Mutant studies disclosed the paramount role of cytochrome bo_3 for growth. In addition, a cytochrome bc_1 complex and cytochrome *c* are present, but presumably no functional cytochrome *c* oxidase. A mutant lacking cytochrome bc_1 showed a growth defect at acidic pH; nevertheless, the precise role of this complex remains to be clarified. Here we present an overview on recent studies concerned with central carbon metabolism and respiration in *G. oxydans* and also discuss corresponding data for species of *Acetobacter* and *Gluconacetobacter*.

Keywords *Gluconobacter oxydans* 621H • Cyclic pentose phosphate pathway • Cytochrome *bd* • Cytochrome bo_3 • Cytochrome bc_1 complex • Genome-wide transcriptome analysis • ^{13}C-Metabolic flux analysis

11.1 Introduction

The strictly aerobic α-proteobacterium *Gluconobacter oxydans* is used for a variety of industrial applications for reasons of its unusual metabolic capabilities, in particular, the incomplete oxidation of organic substrates. The main industrial

S. Bringer (✉) • M. Bott
Institut für Bio- und Geowissenschaften, IBG-1: Biotechnologie, Forschungszentrum Jülich, 52425 Jülich, Germany
e-mail: st.bringer-meyer@fz-juelich.de; m.bott@fz-juelich.de

K. Matsushita et al. (eds.), *Acetic Acid Bacteria*,
DOI 10.1007/978-4-431-55933-7_11

applications of *G. oxydans* are the production of vitamin C, dihydroxyacetone, 6-amino-L-sorbose (a key intermediate for the synthesis of the anti-diabetic drug miglitol), shikimate, and 3-dehydroshikimate (Adachi et al. 2003b; Deppenmeier et al. 2002; Gupta et al. 2001; Macauley et al. 2001; Mamlouk and Gullo 2013; Nishikura-Imamura et al. 2014; Pappenberger and Hohmann 2014; Raspor and Goranovič 2008; Saichana et al. 2015). A set of membrane-integral dehydrogenases enables *G. oxydans* to partially oxidize diverse sugars, sugar alcohols, and other reduced compounds in one or more steps in the periplasm. The resulting products accumulate in the culture medium, often causing its acidification. The catalytic centers of these dehydrogenases are located in the periplasm and deliver electrons or electrons and protons to the respiratory chain (Matsushita et al. 1994, 2004). The rate of these oxidations is usually quite high, resulting in a high demand of *G. oxydans* for oxygen. Only a small fraction of the sugars or sugar alcohols is transported into the cell and catabolized in the cytoplasm via the pentose phosphate pathway (PPP) and the Entner–Doudoroff pathway (EDP). Because of the absence of a gene encoding 6-phosphofructokinase, the Embden–Meyerhof–Parnas pathway (EMP) is nonfunctional (Prust et al. 2005). Similarly, the tricarboxylic acid (TCA) cycle is incomplete because the genes for succinate dehydrogenase and also succinyl-CoA synthetase are lacking. Furthermore, the genome contains neither the key genes of the glyoxylate cycle nor a gene for a gluconeogenetic phosphoenolpyruvate (PEP)-forming enzyme (Deppenmeier and Ehrenreich 2009; Prust et al. 2005).

This chapter summarizes recent studies on central carbon metabolism and respiration in *G. oxydans* 621H (ATCC 621H is identical to DSM2343), including transcriptome analyses with DNA microarrays and ^{13}C-based carbon flux analyses.

11.2 Cytoplasmic Sugar Metabolism

11.2.1 Pentose Phosphate Pathway and the Entner–Doudoroff Pathway

The importance of the PPP and the EDP for cytoplasmic sugar catabolism in *G. oxydans* has long been a matter of interest (Asai 1968; Hauge et al. 1955; Olijve and Kok 1979a, b; Rauch et al. 2010; Shinjoh et al. 1990; Tonouchi et al. 2003). Studies of the dissimilation pathway of L-[U-^{14}C]sorbose by the 2-ketogulonate-producing strain UV10, derived from *Gluconobacter melanogenus* IFO 3293 (now *G. oxydans* NBRC 3293), showed that 40 % of the metabolized substrate was converted to $^{14}CO_2$, which was mainly generated via the PPP (Shinjoh et al. 1990). In vitro characterization of enzymes involved in the central metabolism of *G. oxydans* revealed dual cofactor specificities of the key PPP enzymes glucose 6-phosphate dehydrogenase (GOX0145) and 6-phosphogluconate dehydrogenase (GOX1705). Under physiological conditions, these enzymes were found to be

$NADP^+$- and NAD^+ dependent, respectively (Adachi et al. 1982; Rauch et al. 2010; Tonouchi et al. 2003). Lack of cofactor specificity in the oxidative PPP seemingly is not an uncommon characteristic, as it was also observed in ^{13}C-based metabolic flux analyses of six other bacterial species (Fuhrer and Sauer 2009). Transaldolase (Tal) and glucose 6-phosphate isomerase (Pgi) form a bifunctional enzyme in *G. oxydans* (Sugiyama et al. 2003). Overexpression of the *pgi/tal* gene brought about increased growth rates and final cell densities in strains *G. oxydans* IFO 3293 and *G. oxydans* N44-1 (a derivative of IFO 3293) with sorbitol as the carbon source (Bremus et al. 2008a, b). Furthermore, it was found that the addition of purified Tal-Pgi or ribulokinase increased xylitol production from D-arabitol by a cell-free system of *G. oxydans*, presumably by improving NADH supply via an enhanced activity of the oxidative PPP (Sugiyama et al. 2003).

Recently, an analysis of the cytoplasmic catabolism of fructose formed by oxidation of mannitol, one of the preferred carbon sources of *G. oxydans*, was carried out with a Δ*gnd* mutant lacking 6-phosphogluconate dehydrogenase and thus the oxidative PPP and a Δ*edd-eda* mutant lacking 6-phosphogluconate dehydratase and 2-keto-3-deoxy-6-phosphogluconate aldolase, and thus the EDP (Richhardt et al. 2012). Marker-free gene deletion was accomplished by a method based on *G. oxydans* Δ*upp*, which lacks the *upp* gene for uracil phosphoribosyltransferase (Peters et al. 2013). A scheme of the central carbon metabolism of *G. oxydans*, including the reactions involved in mannitol catabolism, is shown in Fig. 11.1. In the first exponential growth phase, mannitol is oxidized to fructose, which accumulates in the medium. In the second growth phase, part of the fructose is taken up by the cells and another part is oxidized to 5-ketofructose (Fig. 11.2). Growth experiments using media with mannitol as an energy and carbon source and yeast extract as supplement revealed that neither of the two pathways, PPP or EDP, is essential for survival of *G. oxydans*. However, the growth characteristics of the two mutants under controlled conditions showed that the PPP is the main route for cytoplasmic fructose catabolism, whereas the EDP is dispensable and even unfavorable (Fig. 11.2). The Δ*edd-eda* mutant formed 24 % more cell mass than the reference strain. The longer period of almost unimpaired exponential growth of the EDP mutant is probably the result of the lack of an adjustment phase during transition from growth phase I to II. This transition is connected with de novo protein synthesis, as was shown in an earlier study (Olijve and Kok 1979a). In contrast, deletion of *gnd* (6-phosphogluconate dehydrogenase) severely inhibited growth and caused a strong selection pressure for secondary mutations inactivating glucose 6-phosphate dehydrogenase, thus also preventing fructose catabolism via the EDP. These Δ*gnd zwf** mutants were almost totally disabled in fructose catabolism but still produced about 14 % of the carbon dioxide of the reference strain, possibly by catabolizing substrates from the yeast extract. The selection pressure of the Δ*gnd* mutant of *G. oxydans* for secondary *zwf* mutations inactivating glucose 6-phosphate dehydrogenase could be caused by increased concentrations of 6-phosphogluconate or KDPG, which were shown to have an inhibitory effect on growth of *Escherichia coli* (Fuhrman et al. 1998) and *Pseudomonas cepacia* (Allenza and Lessie 1982). Overexpression of *gnd* in the reference strain improved

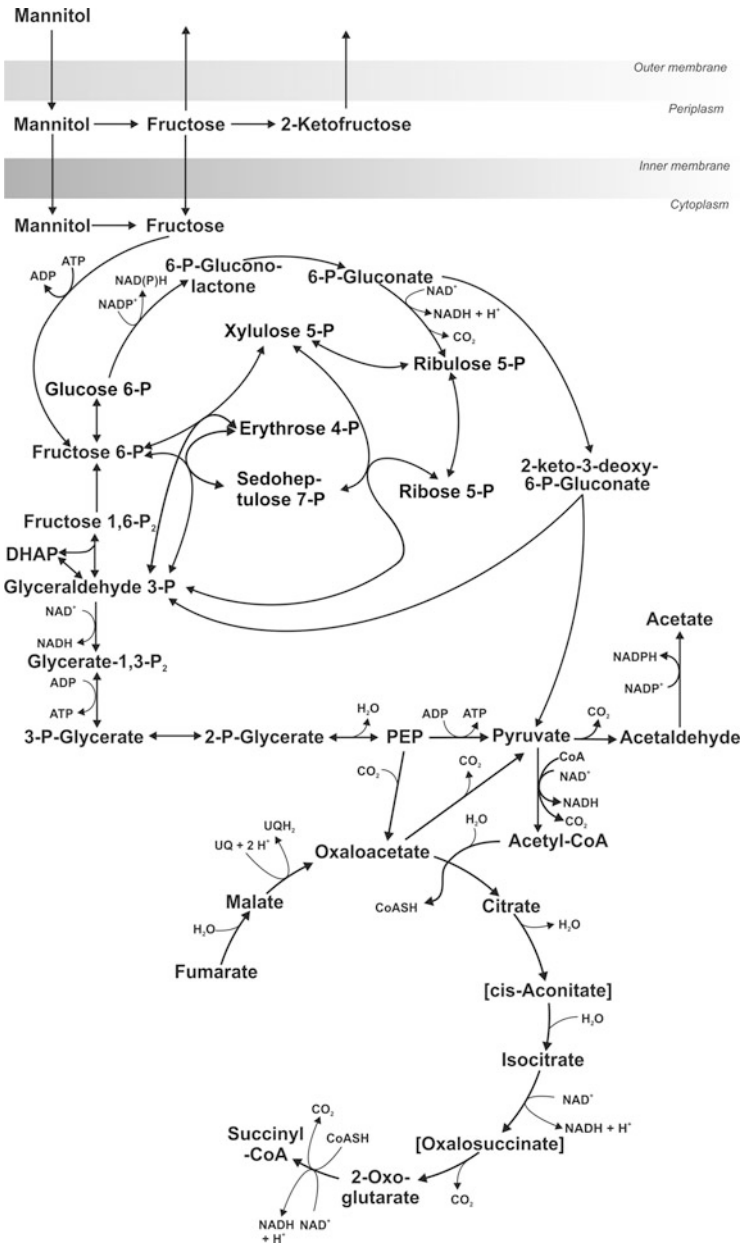

Fig. 11.1 Scheme of the central carbon metabolism of *Gluconobacter oxydans* with the substrate mannitol. *Glucose-6-P* glucose 6-phosphate, *fructose-1,6-P2* fructose 1,6-bisphosphate, *DHAP* dihydroxyacetone phosphate, *UQ* ubiquinone, *PEP* phosphoenolpyruvate

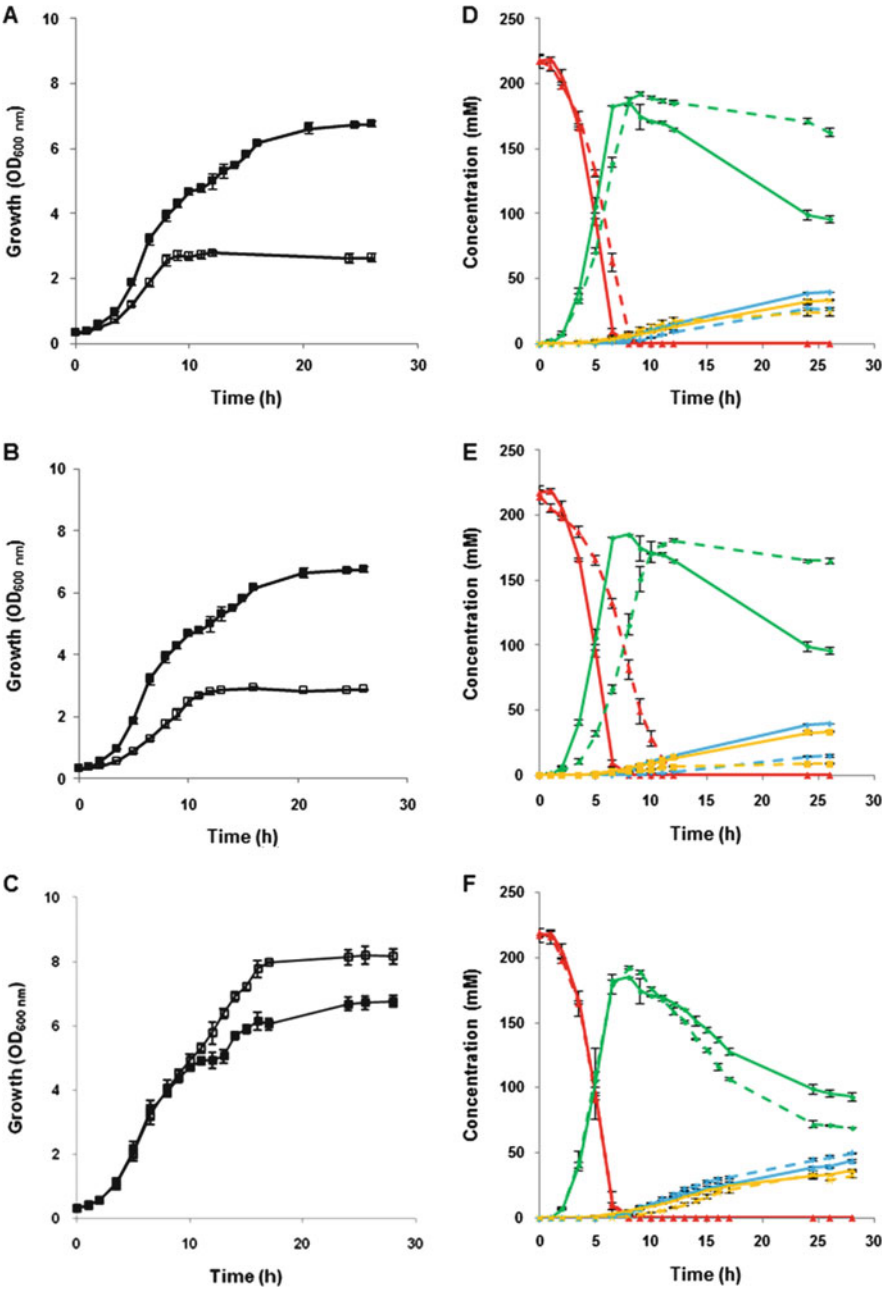

Fig. 11.2 (**a**–**c**) Growth of *G. oxydans* deletion strains (*open symbols*) and the parent strain *G. oxydans* Δ*upp* (*filled symbols*) on mannitol: Δ*gnd* (**a**); Δ*gnd zwf** (**b**); Δ*edd-eda* (**c**). (**d**–**f**) Substrate consumption and product formation of *G. oxydans* deletion strains (*dashed lines*) and the reference strain Δ*upp* (*closed lines*): Δ*gnd* (**d**); Δ*gnd zwf** (**e**); Δ*edd-eda* (**f**). Cells were cultivated in mannitol medium at 15 % dissolved oxygen at pH 6. Mean values and standard deviations of three independent cultures are shown. Mannitol (*red*); fructose (*green*); 5-ketofructose (*blue*); acetate (*yellow*). (Modified from Richhardt et al. 2012)

biomass formation in a manner similar to deletion of *edd-eda*, further confirming the importance of the PPP for cytoplasmic fructose catabolism (Richhardt et al. 2012).

Glucose catabolism by *G. oxydans* proceeds in two phases, comprising rapid periplasmic oxidation of glucose to gluconate together with cytoplasmic 5-ketogluconate production (phase I) followed by periplasmic oxidation of gluconate to 2-ketogluconate and consumption of 5-ketogluconate (phase II) (Fig. 11.3a). Only a small amount of glucose and part of the gluconate are taken up into the cells. To determine the roles of the PPP and the EDP for intracellular glucose and gluconate catabolism, the growth parameters of the mutants Δ*gnd*, Δ*gnd zwf**, and Δ*edd-eda* were determined in a bioreactor at pH 6 and 15 % dissolved oxygen (Richhardt et al. 2013a). In the presence of yeast extract, neither of the two pathways was essential for growth with glucose. However, the PPP mutants showed a reduced growth rate in phase I and completely lacked growth phase II. In contrast, the EDP mutant showed the same growth behavior as the reference strain. These results again demonstrate that the PPP is of major importance for cytoplasmic glucose and gluconate catabolism, whereas the EDP is dispensable. Up to now, the mechanism by which glucose is transported into the cell has not been known for *G. oxydans*. The presence of an incomplete PEP:carbohydrate phosphotransferase system (PTS) lacking the EIIC and EIIB components suggests a regulatory function rather than a transporter function. It was recently shown that the predicted HPr kinase (GOX0816) of *G. oxydans* phosphorylates HPr at Ser54 (Zhang et al. 2014), supporting a regulatory function of the PTS components.

11.2.2 ^{13}C-Metabolic Flux Analyses

The distribution and regulation of periplasmic and cytoplasmic carbon fluxes in *G. oxydans* 621H cultivated on glucose was studied by ^{13}C-based metabolic flux analysis (Hanke et al. 2013). Cells were cultivated with specifically ^{13}C-labeled glucose (Fig. 11.3a), and intracellular metabolites were analyzed for their labeling pattern by liquid chromatography–mass spectrometry (LC-MS). In growth phase I, 90 % of the glucose was oxidized periplasmatically to gluconate and partially further to 2-ketogluconate (Fig. 11.3b). Of the glucose taken up by the cells, 9 % was phosphorylated to glucose 6-phosphate, whereas 91 % was oxidized by cytoplasmic glucose dehydrogenase to gluconate (Fig. 11.3b, c). Of the gluconate formed in this way or taken up into the cells by a gluconate permease (GOX2188), 70 % was oxidized to 5-ketogluconate and 30 % was phosphorylated to 6-phosphogluconate. In growth phase II, 87 % of gluconate was oxidized to 2-ketogluconate in the periplasm and 13 % was taken up by the cells and almost completely converted to 6-phosphogluconate (Fig. 11.3b, c). ^{13}C-Metabolic flux analysis (MFA) showed that 6-phosphogluconate is catabolized primarily via the oxidative PPP in both phase I and II (62 % and 93 %, respectively), and

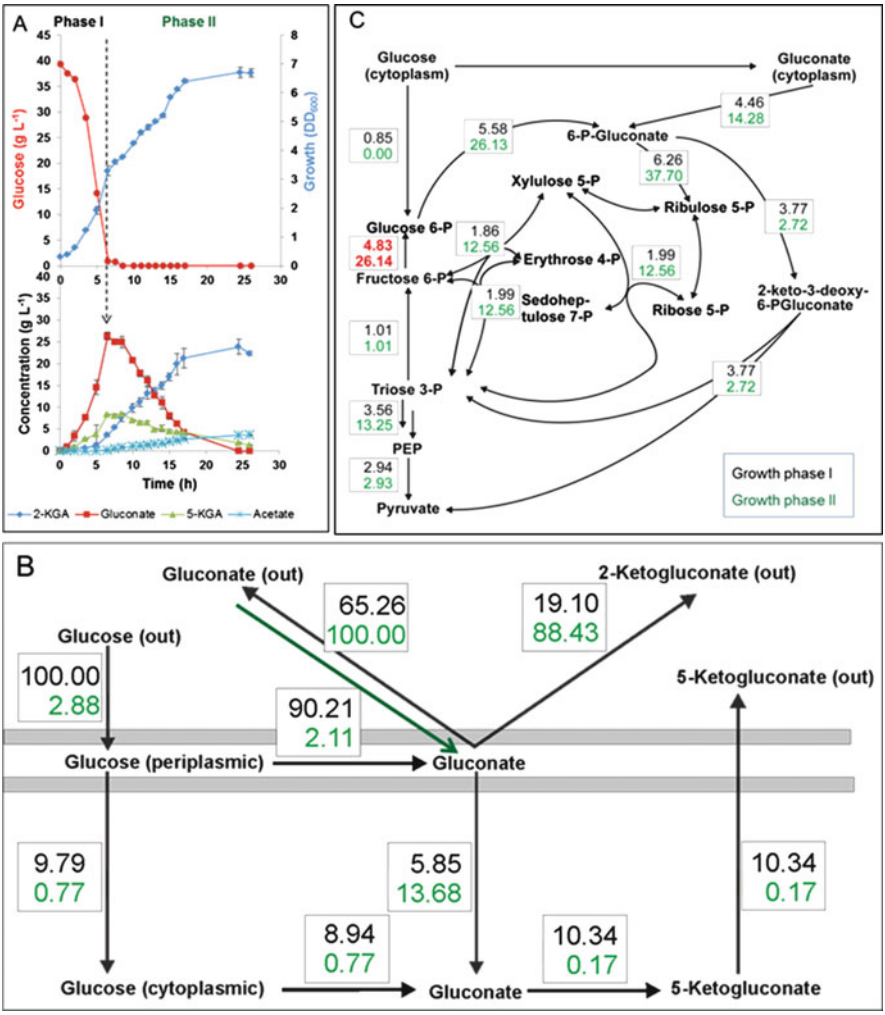

Fig. 11.3 ^{13}C-Metabolic flux analysis of *G. oxydans* during growth on glucose. **a** Growth (optical density at 600 nm) and glucose consumption (*upper graph*), product formation and consumption (*lower graph*). **b** Periplasmic and cytoplasmic carbon fluxes of nonphosphorylated intermediates. **c** Cytoplasmic carbon fluxes in central metabolism during growth phases I and II. Flux values given in **b** and **c** are related to 100 % glucose uptake (growth phase I) or 100 % gluconate uptake (growth phase II)

demonstrated a cyclic carbon flux through the oxidative PPP, as shown by the positive flux from fructose 6-phosphate to glucose 6-phosphate (indicated in red in Fig. 11.3c).

A cyclic operation of the PPP, as shown for *G. oxydans*, was also observed for *Gluconacetobacter (Ga.) oboediens* (recently renamed as *Komagataeibacter oboediens*) and *Gluconacetobacter xylinus* (recently renamed as *Komagataeibacter*

xylinus) (Sarkar et al. 2010; Zhong et al. 2013). Carbon flux analyses with *Ga. oboediens* cultivated on glucose (15 g l^{-1}) and acetate (5.24 g l^{-1}) by ^{13}C-labeling experiments showed that in spite of the presence of a *pfk* gene encoding phosphofructokinase, the activity of this enzyme was very low, leading to a negative carbon flux through the phosphoglucose isomerase (Pgi)-catalyzed reaction (i.e., a positive flux from fructose 6-phosphate to glucose 6-phosphate) and cyclization of the oxidative PPP (Sarkar et al. 2010). The same was observed in another study with *Ga. xylinus*, where negative fluxes through Pgi were determined in cells grown on the carbon sources glucose, fructose, and glycerol (Zhong et al. 2013).

Cocoa bean fermentation is a mixed-culture process, consisting initially of fermentations by yeast and lactic acid bacteria followed by oxidation of the fermentation products ethanol and lactic acid into acetic acid and acetoin by several *Acetobacter* strains, of which *A. pasteurianus* is the prominent one (Moens et al. 2014). A ^{13}C-based carbon flux analysis of *Acetobacter* during cocoa pulp fermentation-simulating conditions revealed a functionally separated metabolism during co-consumption of ethanol and lactate. Acetate was almost exclusively derived from ethanol, whereas lactate served for formation of acetoin and biomass building blocks. This switch was attributed to the lack of phosphoenolpyruvate carboxykinase and malic enzyme activities, which prevents conversion of oxaloacetate and malate formed by acetate metabolism in the TCA cycle to PEP and pyruvate and subsequently to acetoin (Adler et al. 2014). Lactate, on the other hand, can be converted to pyruvate, which is then used for acetoin formation or, after conversion to PEP by pyruvate phosphate dikinase, for gluconeogenesis. The inability of conversion of TCA cycle intermediates to PEP resembles the situation in *G. oxydans*, where in addition no enzyme for conversion of pyruvate to PEP is present.

11.2.3 Transcriptome Analyses

For a better understanding of the two growth phases observed for *G. oxydans* during cultivation on glucose, a transcriptome comparison was performed using RNA isolated from cells harvested in phase I and phase II (Hanke et al. 2013). The DNA microarray analyses revealed 454 genes showing differential expression: 227 genes had an mRNA ratio (phase II/phase I) $\geq$2.0, and 227 genes had an mRNA ratio $\leq$0.5 (Hanke et al. 2013). Several genes encoding proteins that feed electrons into the respiratory chain showed increased mRNA levels in phase II, such as those for a PQQ-containing *myo*-inositol dehydrogenase (GOX1857), for the membrane-bound gluconate 2-dehydrogenase (GOX1230 and GOX1231), and for the type II NADH dehydrogenase (GOX1675). One of the two terminal oxidases of the respiratory chain of *G. oxydans*, the cytochrome *bd* ubiquinol oxidase, renamed "cyanide-insensitive oxidase CIO" (GOX0278 and GOX0279) (Miura et al. 2013), was also upregulated in growth phase II. The genes encoding the membrane-integral pyridine nucleotide transhydrogenase (*pntA1A2B*, GOX0310-0312)

belonged to the most strongly upregulated genes in phase II. The genes downstream of *pntB*, GOX0313 and GOX0314, encode putative alcohol dehydrogenases and showed comparable mRNA ratios as the *pntA1A2B* genes. The *G. oxydans* genome contains three gene clusters coding for subunits of F_1F_o-ATP synthases. The clusters GOX1110 to GOX1113 and GOX1310 to GOX1314 encode the subunits of the F_o part and the F_1 part of an ATP synthase, which is an orthologue of the ATP synthases of *Acetobacter pasteurianus* IFO 3283-01, *Gluconacetobacter diazotrophicus* PAL 5, and other *α-Proteobacteria*. Both these clusters showed decreased expression in phase II. The genes of the third cluster, GOX2167 to GOX 2175, might code for a Na^+-translocating F_1F_o-ATP synthase (Dibrova et al. 2010), and showed an increased expression in phase II. Furthermore, the DNA microarray analysis revealed an increased expression of PPP genes in growth phase II, which correlated with an increased PPP flux in phase II. Moreover, genes possibly related to a general stress response displayed increased expression in growth phase II (Hanke et al. 2013).

Transcriptome studies aimed at understanding the influence of different carbon sources on global gene expression were also performed for *A. aceti* NBRC 14818 cultivated on either ethanol, or acetate, or glucose, or a mixture of ethanol and glucose (Sakurai et al. 2011). In contrast to *G. oxydans*, this species possesses all genes for the TCA cycle as well as the glyoxylate cycle and thus is able to completely oxidize ethanol and acetate and perform anaplerosis. Neither the gene for phosphofructokinase nor that for 2-keto-3-deoxy-6-phosphogluconate aldolase could be identified, suggesting that sugar catabolism presumably proceeds exclusively via the PPP. As genes for acetate kinase and phosphotransacetylase are absent, acetate activation occurs either via acetyl-CoA synthetase, for which two genes are present, or via succinyl-CoA:acetate CoA transferase. Growth on ethanol is diauxic, whereby in the first phase ethanol is oxidized to acetate and in the second phase acetate is oxidized to CO_2. Glucose (40 g/l) was almost completely oxidized to the end product gluconate, and biomass formation was much lower than with 10 g/l ethanol, suggesting that the strain is unable to efficiently utilize glucose and gluconate as carbon and energy sources. The transcriptome studies revealed a variety of carbon source-specific responses. The TCA cycle genes displayed higher mRNA levels during growth on acetate or glucose than on ethanol or ethanol/glucose mixture. The glyoxylate cycle genes showed high expression during growth on ethanol, acetate, and the glucose/ethanol mixture, but were not expressed on glucose alone, in accord with the known function of this pathway. Ethanol triggered increased expression of several stress-responsive genes.

In a further study, the time-dependent transcriptome changes during cultivation of *A. aceti* NBRC 14818 on ethanol were analyzed (Sakurai et al. 2012). In line with the previous data, the TCA cycle genes showed low mRNA levels during oxidation of ethanol to acetate and were significantly upregulated in the transition and acetate oxidation phases. This result suggested that the switch from acetate accumulation to acetate oxidation might be controlled by changes in the metabolic flux through the TCA cycle.

11.3 Respiratory Energy Metabolism

Because its many membrane-bound dehydrogenases incompletely oxidize sugars, sugar alcohols, and other compounds stereo- and regioselectively in the periplasm, *Gluconobacter oxydans* has been used for decades in industrial biotechnology (Adachi et al. 2003a; De Ley et al. 1984; Matsushita et al. 1994, 2002, 2004; Saichana et al. 2015; Yakushi and Matsushita 2010). The membrane-bound dehydrogenases transfer the reducing equivalents to ubiquinone. Two quinol oxidases, cytochrome bo_3 and cytochrome *bd*, then catalyze transfer of the electrons from ubiquinol to molecular oxygen (Fig. 11.4). Based on the cyanide insensitivity of *G. oxydans* cytochrome *bd*, Matsushita and coworkers designated this enzyme as cyanide-insensitive oxidase CIO and the corresponding genes *cioA* and *cioB* instead of *cydA* and *cydB* (Mogi et al. 2009). In a recent study, they purified and characterized the terminal oxidases of *G. oxydans* and for comparison cytochrome *bd* of *Escherichia coli* (Miura et al. 2013) (cf. Chaps. 7 and 13, in this volume). Based on the reported data, a different designation for members of the CIO clade, *cioAB*, is used in the following text (Fig. 11.4).

11.3.1 Roles of the Two Terminal Oxidases Cytochrome bo_3 *and Cyanide-Insensitive Oxidase, CIO*

To elucidate the role of the two terminal oxidases of *G. oxydans*, the in-frame deletion mutants Δ*cioAB* (previously termed Δ*cydAB*) and Δ*cyoBACD* were constructed and characterized with respect to growth, respiratory activity, and H^+/O ratio (Richhardt et al. 2013b). Deletion of the *cioAB* genes had no obvious influence on growth, whereas the lack of the *cyoBACD* genes severely reduced the growth rate and the cell yield. Using a respiration activity monitoring system and adjusting different levels of oxygen availability, hints for a low oxygen affinity of CIO were obtained, which were supported by measurements of oxygen consumption in a respirometer. Our evidence that CIO of *G. oxydans* has a significantly lower oxygen affinity than cytochrome bo_3 oxidase is in agreement with recent biochemical data, wherein the K_m values for oxygen of CIO and cytochrome bo_3 determined with oxymyoglobin were reported to be 21 μM and 3 μM, respectively (Miura et al. 2013).

The H^+/O ratio of the Δ*cyoBACD* mutant with mannitol as substrate was 0.56 ± 0.11, and more than 50 % lower than that of the reference strain (1.26 ± 0.06) and the Δ*cioAB* mutant (1.31 ± 0.16), indicating that cytochrome bo_3 oxidase is the main component for proton extrusion via the respiratory chain (Richhardt et al. 2013b). In previous studies, H^+/O ratios of 1.7–2.2 were reported for *G. oxydans* cells supplied with glycerol, glucose, lactate, or ethanol at pH 6 (Matsushita et al. 1989). The differences could be caused by the use of other substrates or differences in the experimental conditions. For cytochrome bo_3

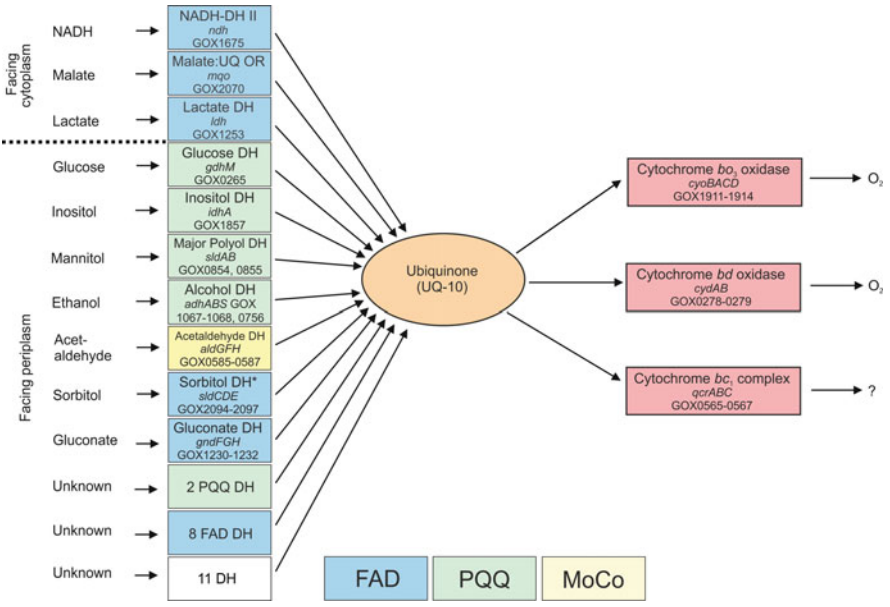

Fig. 11.4 Overview of the components of the respiratory chain of *G. oxydans* 621H. *DH* dehydrogenase, *FAD* flavin adenine dinucleotide, *PQQ* pyrroloquinoline quinone, *MoCo* molybdopterin cofactor, *CIO* cyanide-insensitive oxidase. *In the sequenced strain 621H, the *sldD* gene encoding the flavoprotein subunit of the sorbitol dehydrogenase contains a frameshift mutation in codon 70, resulting in fragmentation (GOX2095, GOX2096) and the absence of 30 amino acids (positions 70–100 in the native SldD protein) (Prust et al. 2005). The functionality of the resulting complex is therefore questionable. (Modified from Richhardt et al. 2013b)

oxidase, an H^+/e stoichiometry of 2 and therefore an H^+/O ratio of 4 can be assumed (Puustinen et al. 1989), and for cytochrome *bd* oxidase an H^+/e stoichiometry of 1 and an H^+/O ratio of 2 (Jasaitis et al. 2000; Puustinen et al. 1991). As the CIO was not relevant for growth of *G. oxydans* and proton translocation under the conditions used by Richhardt et al. 2013b, a H^+/O ratio approaching 4 might be expected for *G. oxydans*. However, both our results as well as those presented by Matsushita et al. 1989 are much lower than a value of 4. There are a number of very speculative hypotheses to explain the low H^+/O ratios determined for *G. oxydans*. (1) The cytoplasmic membrane of *G. oxydans* might be more leaky for protons than that of *E. coli*, causing a non-energy-conserving backflow of protons into the cells (Brown 1992). (2) The respiratory chain could involve a reverse electron transfer coupled to an influx of protons (van der Oost et al. 1995). (3) Cytochrome bo_3 oxidase might not function as a primary proton pump, but as a Na^+ pump, as has been described for cytochrome bo_3 oxidase of *Vitreoscilla* sp. (Kim et al. 2005; Park et al. 1996). In this context it is interesting to note that *G. oxydans* possesses two different F_1F_o-type ATP synthases (Dibrova et al. 2010), one of which might use Na^+ as the coupling ion (Hanke et al. 2012; Prust et al. 2005). The comparative DNA microarray analysis of the *cyoBACD* deletion mutant versus the reference strain showed

an upregulation of genes (GOX2167-2175) coding for the putative Na^+-dependent F_1F_o-ATPase (Richhardt et al. 2013b).

Plasmid-based overexpression of *cyoBACD* led to increased growth rates and growth yields in both the wild type and the Δ*cyoBACD* mutant, suggesting that cytochrome bo_3 might be a rate-limiting factor of the respiratory chain (Richhardt et al. 2013b). Although additional studies are required to clarify the positive effect of cytochrome bo_3 overproduction, the result shows that respiratory chain components are a promising starting point for further optimization of *G. oxydans* for its use in biotechnological applications. Recently, a comparison of the genome sequences of *G. oxydans* 621H and *G. oxydans* DSM 3504 revealed, among others, the presence of an additional type II NADH dehydrogenase gene (*ndh2*) in strain DSM3504, which reaches an optical density almost three times higher than that of *G. oxydans* 621H. Interestingly, plasmid-based expression of *ndh2* from strain DSM3504 in strain 621H led to a significantly increased growth rate (Kostner et al. 2014), explained by a competition between membrane-bound dehydrogenases and NADH dehydrogenase for transferring electrons to ubiquinone, which could be altered in favor of the latter enzyme by increased *ndh* expression.

11.3.2 Influence of Oxygen on Global Gene Expression

G. oxydans is strictly aerobic; nevertheless, in its natural habitat, oxygen deprivation caused by the rapid oxygen consumption by *G. oxydans* itself is likely to occur very often. In a recent study, the genome-wide transcriptional responses of *G. oxydans* 621H to oxygen limitation were analyzed (Hanke et al. 2012). For that purpose, cells were cultivated in a bioreactor system for 6 h at a constant dissolved oxygen concentration (DOC) of 15 %, before gassing was switched to a mixture of 2 % O_2 and 98 % N_2, leading to a DOC of 0 %. Samples for RNA isolation were taken before and 4 h after the switch and used for comparative transcriptome analysis with DNA microarrays. Oxygen deprivation caused expression changes of almost 500 genes, 215 with a $\geq$2.0-fold increased and 271 with a $\geq$2.0-fold decreased mRNA ratio (oxygen limitation/oxygen excess). Accordingly, oxygen limitation triggered a strong response influencing transcription of about 20 % of all chromosomal genes, including many involved in respiration and oxidative phosphorylation.

Although several genes coding for respiratory dehydrogenases showed reduced mRNA levels, expression of the terminal oxidase genes was increased. An opposite regulation of the dehydrogenases, several of which are PQQ dependent, and the terminal oxidases represents an adequate response to oxygen limitation, as it probably allows the cells to reduce the electron flux into the respiratory chain on the one hand and to increase the capability to capture the limiting oxygen on the other. The reduced expression of genes involved in PQQ biosynthesis and the increased expression of genes required for heme biosynthesis fits the expression patterns of the dehydrogenases and the terminal oxidases.

The genes for the membrane-integral pyridine nucleotide transhydrogenase PntA1A2B were among the most strongly upregulated genes under oxygen limitation (10- to 15 fold). The enzyme either consumes the electrochemical proton gradient Δp for $NADP^+$ reduction or generates Δp at the expense of NADPH oxidation (Jackson et al. 2002). As observed in another study (see earlier), the genes downstream of *pntA1A2B* (GOX0313, GOX0314) encoding putative zinc-containing alcohol dehydrogenases showed mRNA ratios similar to the *pntA1A2B* genes, suggesting that these five genes might form an operon and a functional connection between the encoded enzymes. Increased levels of these enzymes might allow the cells a rapid exchange between NAD^+/NADH and $NADP^+$/NADPH and reoxidation of NAD(P)H via reduction of aldehydes/ketones to the corresponding alcohols, which could be favorable under oxygen limitation. In fact, the enzyme encoded by GOX0313 was recently shown to function as medium-chain alcohol dehydrogenase oxidizing various primary alcohols, but having a preference for substrate reduction, reducing many aldehydes and α-diketones (Schweiger et al. 2013).

As mentioned previously, the *G. oxydans* genome contains genes for two F_1F_o-ATP synthases, one of which might code for a Na^+-translocating F_1F_o-ATP synthase. The genes for the presumably H^+-translocating F_1F_o-ATP synthase showed a decreased expression under oxygen limitation, whereas those for the putative Na^+-translocating enzyme had increased mRNA levels. Remarkably, an inverse regulation of the two F_1F_o-ATP synthases was also observed in the transcriptome comparison of growth phase I and II during cultivation of *G. oxydans* on glucose (see earlier). Many genes encoding proteins involved in transcription and translation showed lower expression under oxygen limitation, including subunits of the RNA polymerase, elongation factors, and 45 ribosomal proteins. This response probably presents an adaptation to the reduced linear growth observed after shifting the cells from oxygen excess to oxygen limitation. Overall, the transcriptome comparison revealed a complex response of *G. oxydans* to oxygen starvation and raised many interesting questions that deserve more detailed studies, such as the function of the two inversely regulated F_1F_o-ATP synthases.

11.3.3 The Enigmatic Function of the Cytochrome bc_1 *Complex*

G. oxydans possesses the genes *qcrABC* (GOX0565-0567) for a cytochrome bc_1 complex, *cycA* (GOX0258) for a soluble cytochrome c_{552}, GOX1863 for a protein with similarity to subunit I of cytochrome *c* oxidase, and *ctaB* (GOX1864) for heme *o*-synthetase (Matsutani et al. 2014; Prust et al. 2005; Sakurai et al. 2011). As the putative subunit I lacks histidine residues serving as Cu_B and heme a_3 ligands, it is unlikely to be functional. Moreover, genes for subunits II and III of cytochrome

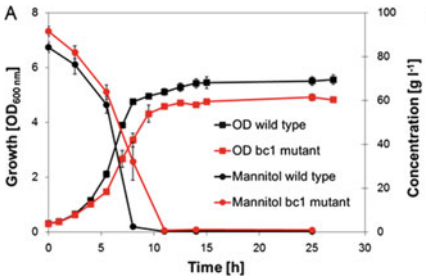

B

Annotation	Gene	I	II
Respiration and ATP synthesis			
NAD(P) transhydrogenase SUα2	*pntA2*	3.14	10.37
NAD(P) transhydrogenase SUα1	*pntA1*	3.80	14.70
NAD(P) transhydrogenase SUβ	*pntB*	3.44	12.04
Alcohol:NAD$^+$oxidoreductase SUα	*adhA*	4.00	13.58
Alcohol:NAD$^+$oxidoreductase SUβ	*adhB*	3.58	14.63
Cytochrome bo_3 ubiquinol oxidase SUII	*cyoB*	2.09	2.82
Cytochrome bo_3 ubiquinol oxidase SUI	*cyoA*	2.28	2.70
Cytochrome bo_3 ubiquinol oxidase SUIII	*cyoC*	2.10	3.56
Cytochrome bo_3 ubiquinol oxidase SUIV	*cyoD*	2.15	3.81

Fig. 11.5 (**a**) Growth and substrate consumption of *G. oxydans* 621H wild type and the cytochrome bc_1 mutant Δ*qcrABC* at pH 4 on 80 g l^{-1} mannitol under oxygen saturation. (**b**) Selected mRNA ratios from two different DNA microarray experiments: *I*, strain Δ*qcrABC* versus wild type, both cultivated at pH 4 under oxygen saturation; *II*, wild type cultivated under oxygen limitation versus wild type cultivated under oxygen saturation, both at pH 6. Genes shown are an excerpt of 51 genes having identical regulation patterns. (**a** was modified from Hanke et al. 2012)

c oxidase are absent in the genome. To understand the function of a cytochrome bc_1 complex in the presumptive absence of a functional cytochrome *c* oxidase, a Δ*qcrABC* mutant of *G. oxydans* was constructed and analyzed (Hanke et al. 2012). Although the mutant showed the same growth behavior as the wild type during cultivation on mannitol at pH 6, a growth defect was observed at pH 4 under oxygen saturation, where the mutant showed a 18 % reduced growth rate and a 13 % lower final optical density. Comparison of the transcriptomes of the Δ*qcrABC* mutant versus the wild type at pH 4 revealed 51 differentially expressed genes. Interestingly, almost all the 45 genes with increased expression in the Δ*qcrABC* mutant at pH 4 (including the cytochrome bo_3 oxidase genes) were also upregulated in the wild type grown at pH 6 under oxygen limitation (Fig. 11.5). The results obtained for the Δ*qcrABC* mutant clearly suggest that the cytochrome bc_1 complex possesses a physiological function in *G. oxydans*, at least at acidic pH, but further studies are required to elucidate this function.

Two sets of genes for the cytochrome bc_1 complex, one of which lacks the gene for the Rieske iron sulfur protein, were identified in *Acetobacter aceti* NBRC 14818 and *A. pasteurianus* NBRC 3283 (Azuma et al. 2009; Sakurai et al. 2011). In both species also a gene encoding a putative subunit I of cytochrome *c* oxidase (*coxA*) was identified, but genes for subunits II and III were absent in the genome (Sakurai et al. 2011). Further organisms containing the genes for a cytochrome bc_1 complex but presumably lacking a functional cytochrome *c* oxidase are *Acetobacter pasteurianus* 386B (Illeghems et al. 2013) and *Zymomonas mobilis* (Balodite et al. 2014; Charoensuk et al. 2011; Sootsuwan et al. 2008), all of which belong to the *α-Proteobacteria*. Accordingly, this situation is not specific for *G. oxydans*, but is widespread in related bacteria.

One idea regarding the function of the cytochrome bc_1 complex is to provide reduced cytochrome *c* for reduction of hydrogen peroxide to water by an enzyme called cytochrome *c* peroxidase. *G. oxydans* (GOX0998) and many other acetic acid bacteria with known genome sequences possess the corresponding *ccpR* gene.

However, both in *G. oxydans* and in *A. aceti* NBRC 14818, the expression level of *ccpR* was low under the conditions tested (Hanke et al. 2012; Sakurai et al. 2011). In other bacteria, these enzymes are usually present in addition to other terminal electron acceptors for reduced cytochrome *c* (Atack and Kelly 2007) and there is currently no experimental evidence for such a function of the cytochrome bc_1 complex in the aforementioned species.

11.4 Concluding Remarks

In the past years, a more detailed understanding of the metabolic features of *G. oxydans* and several other acetic acid bacteria was obtained based on the availability of genome sequences, the application of omics technologies such as transcriptomics and fluxomics, and by the detailed analysis of defined mutants. The genome sequences revealed significant heterogeneity in the equipment of individual species with membrane-bound dehydrogenases, sugar catabolic pathways, the TCA cycle, and the glyoxylate cycle. These differences are reflected in the metabolic properties of the species. *Gluconobacter oxydans* is one of the acetic acid bacteria prominently applied in industrial production processes, which are often whole-cell biotransformations requiring prior biomass production. Because the cell yield of *G. oxydans* (0.09 $g_{cdw}/g_{glucose}$ during bioreactor cultivation is very low (Krajewski et al. 2010; Richhardt et al. 2013a), biomass production is cost intensive and presents a disadvantage for industrial application. The results obtained in the studies summarized here disclose starting points for improving the biomass yield and broadening the application range of *G. oxydans* by metabolic engineering of cytoplasmic sugar catabolism and respiratory energy metabolism.

Acknowledgments We are most grateful to Armin Ehrenreich and Wolfgang Liebl (Technical University of Munich, Germany) for providing the strains and protocols used for generating the *G. oxydans* deletion mutants. We thank Jayne Louise Wilson (The University of Sheffield, United Kingdom) for advising us on the method of H^+/O measurement. We thank Petra Simić, Dietmar Laudert, Günter Pappenberger, and Hans-Peter Hohmann (DSM Nutritional Products) for their scientific input and their continued disposition for discussion.

We also thank DSM Nutritional Products (Kaiseraugst, Switzerland) for financial support. This work was funded by the German Ministry of Education and Research (BMBF) within the GenoMik-Plus and GenoMik-Transfer programs (grants 0313751H and 0315632D).

References

Adachi O, Osada K, Matsushita K, Shinagawa E, Ameyama M (1982) Purification, crystallization and properties of 6-phospho- D-gluconate dehydrogenase from *Gluconobacter suboxydans*. Agric Biol Chem 46:391–398

Adachi O, Moonmangmee D, Shinagawa E, Toyama H, Yamada M, Matsushita K (2003a) New quinoproteins in oxidative fermentation. Biochim Biophys Acta 1647:10–17

Adachi O, Moonmangmee D, Toyama H, Yamada M, Shinagawa E, Matsushita K (2003b) New developments in oxidative fermentation. Appl Microbiol Biotechnol 60:643–653

Adler P, Frey LJ, Berger A, Bolten CJ, Hansen CE, Wittmann C (2014) The key to acetate: metabolic fluxes of acetic acid bacteria under cocoa pulp fermentation simulating conditions. Appl Environ Microbiol 80:4702–4716

Allenza P, Lessie TG (1982) *Pseudomonas cepacia* mutants blocked in the Entner-Doudoroff pathway. J Bacteriol 150:1340–1347

Asai T (1968) Acetic acid bacteria: classification and biochemical activities. University of Tokyo Press, Tokyo

Atack JM, Kelly DJ (2007) Structure, mechanism and physiological roles of bacterial cytochrome *c* peroxidases. Adv Microb Physiol 52:73–106

Azuma Y, Hosoyama A, Matsutani M, Furuya N, Horikawa H, Harada T, Hirakawa H, Kuhara S, Matsushita K, Fujita N, Shirai M (2009) Whole-genome analyses reveal genetic instability of *Acetobacter pasteurianus*. Nucleic Acids Res 37:5768–5783

Balodite E, Strazdina I, Galinina N, Mclean S, Rutkis R, Poole RK, Kalnenieks U (2014) Structure of the *Zymomonas mobilis* respiratory chain: oxygen affinity of electron transport and the role of cytochrome *c* peroxidase. Microbiology 160:2045–2052

Bremus C, Bringer-Meyer S, Hermann U, Mouncey NJ, Sahm H (2008a) Biological process using a glucose-6-phosphate isomerase. Google patents EP1873248A1

Bremus C, Bringer-Meyer S, Hermann U, Mouncey NJ, Sahm H (2008b) Biological process using a transaldolase. Google patents EP1873246 A1

Brown GC (1992) The leaks and slips of bioenergetic membranes. FASEB J 6:2961–2965

Charoensuk K, Irie A, Lertwattanasakul N, Sootsuwan K, Thanonkeo P, Yamada M (2011) Physiological importance of cytochrome *c* peroxidase in ethanologenic thermotolerant *Zymomonas mobilis*. J Mol Microbiol Biotechnol 20:70–82

De Ley J, Gillis M, Swings J (1984) The genus *Gluconobacter*. In: Krieg NR, Holt JG (eds) Bergey's manual of systematic bacteriology. Williams & Wilkins, Baltimore, pp 267–278

Deppenmeier U, Ehrenreich A (2009) Physiology of acetic acid bacteria in light of the genome sequence of *Gluconobacter oxydans*. J Mol Microbiol Biotechnol 16:69–80

Deppenmeier U, Hoffmeister M, Prust C (2002) Biochemistry and biotechnological applications of *Gluconobacter* strains. Appl Microbiol Biotechnol 60:233–242

Dibrova DV, Galperin M, Mulkidjanian A (2010) Characterization of the N-ATPase, a distinct, laterally transferred Na^+-translocating form of the bacterial F-type membrane ATPase. Bioinformatics 26:1473–1476

Fuhrer T, Sauer U (2009) Different biochemical mechanisms ensure network-wide balancing of reducing equivalents in microbial metabolism. J Bacteriol 191:2112–2121

Fuhrman LK, Wanken A, Nickerson KW, Conway T (1998) Rapid accumulation of intracellular 2-keto-3-deoxy-6-phosphogluconate in an Entner–Doudoroff aldolase mutant results in bacteriostasis. FEMS Microbiol Lett 159:261–266

Gupta A, Singh VK, Qazi GN, Kumar A (2001) *Gluconobacter oxydans*: its biotechnological applications. J Mol Microbiol Biotechnol 3:445–456

Hanke T, Richhardt J, Polen T, Sahm H, Bringer S, Bott M (2012) Influence of oxygen limitation, absence of the cytochrome bc_1 complex and low pH on global gene expression in *Gluconobacter oxydans* 621H using DNA microarray technology. J Biotechnol 157:359–372

Hanke T, Nöh K, Noack S, Polen T, Bringer S, Sahm H, Wiechert W, Bott M (2013) Combined fluxomics and transcriptomics analysis of glucose catabolism via a partially cyclic pentose phosphate pathway in *Gluconobacter oxydans* 621H. Appl Environ Microbiol 79:2336–2348

Hauge JG, King TE, Cheldelin VH (1955) Oxidation of dihydroxyacetone via the pentose cycle in *Acetobacter suboxydans*. J Biol Chem 214:11–26

Illeghems K, De Vuyst L, Weckx S (2013) Complete genome sequence and comparative analysis of *Acetobacter pasteurianus* 386B, a strain well-adapted to the cocoa bean fermentation ecosystem. BMC Genomics 14:526

Jackson JB, White SA, Quirk PG, Venning JD (2002) The alternating site, binding change mechanism for proton translocation by transhydrogenase. Biochemistry 41:4173–4185

Jasaitis A, Borisov VB, Belevich NP, Morgan JE, Konstantinov AA, Verkhovsky MI (2000) Electrogenic reactions of cytochrome *bd*. Biochemistry 39:13800–13809

Kim SK, Stark BC, Webster DA (2005) Evidence that Na^+-pumping occurs through the D-channel in *Vitreoscilla* cytochrome *bo*. Biochem Biophys Res Commun 332:332–338

Kostner D, Luchterhand B, Junker A, Volland S, Daniel R, Büchs J, Liebl W, Ehrenreich A (2014) The consequence of an additional NADH dehydrogenase paralog on the growth of *Gluconobacter oxydans* DSM3504. Appl Microbiol Biotechnol 99(1):375–386. doi:10.1007/s00253-014-6069-9

Krajewski V, Simić P, Mouncey NJ, Bringer S, Sahm H, Bott M (2010) Metabolic engineering of *Gluconobacter oxydans* for improved growth rate and growth yield on glucose by elimination of gluconate formation. Appl Environ Microbiol 76:4369–4376

Macauley S, Mcneil B, Harvey LM (2001) The genus *Gluconobacter* and its applications in biotechnology. Crit Rev Biotechnol 21:1–25

Mamlouk D, Gullo M (2013) Acetic acid bacteria: physiology and carbon sources oxidation. Indian J Microbiol 53:377–384

Matsushita K, Nagatani Y, Shinagawa E, Adachi O, Ameyama M (1989) Effect of extracellular pH on the respiratory chain and energetics of *Gluconobacter suboxydans*. Agric Biol Chem 53:2895–2902

Matsushita K, Toyama H, Adachi O (1994) Respiratory chains and bioenergetics of acetic acid bacteria. Adv Microb Physiol 36:247–301

Matsushita K, Toyama H, Yamada M, Adachi O (2002) Quinoproteins: structure, function, and biotechnological applications. Appl Microbiol Biotechnol 58:13–22

Matsushita K, Toyama H, Adachi O (2004) Respiratory chains in acetic acid bacteria: membrane bound periplasmic sugar and alcohol respirations. In: Respiration in Archaea and Bacteria. Advances in photosynthesis and respiration. Springer, Dordrecht, pp 81–99

Matsutani M, Fukushima K, Kayama C, Arimitsu M, Hirakawa H, Toyama H, Adachi O, Yakushi T, Matsushita K (2014) Replacement of a terminal cytochrome *c* oxidase by ubiquinol oxidase during the evolution of acetic acid bacteria. Biochim Biophys Acta 1837:1810–1820

Miura H, Mogi T, Ano Y, Migita CT, Matsutani M, Yakushi T, Kita K, Matsushita K (2013) Cyanide-insensitive quinol oxidase (CIO) from *Gluconobacter oxydans* is a unique terminal oxidase subfamily of cytochrome *bd*. J Biochem (Tokyo) 153:535–545

Moens F, Lefeber T, De Vuyst L (2014) Oxidation of metabolites highlights the microbial interactions and role of *Acetobacter pasteurianus* during cocoa bean fermentation. Appl Environ Microbiol 80:1848–1857

Mogi T, Ano Y, Nakatsuka T, Toyama H, Muroi A, Miyoshi H, Migita CT, Ui H, Shiomi K, Omura S, Kita K, Matsushita K (2009) Biochemical and spectroscopic properties of cyanide-insensitive quinol oxidase from *Gluconobacter oxydans*. J Biochem (Tokyo) 146:263–271

Nishikura-Imamura S, Matsutani M, Insomphun C, Vangnai AS, Toyama H, Yakushi T, Abe T, Adachi O, Matsushita K (2014) Overexpression of a type II 3-dehydroquinate dehydratase enhances the biotransformation of quinate to 3-dehydroshikimate in *Gluconobacter oxydans*. Appl Microbiol Biotechnol 98:2955–2963

Olijve W, Kok JJ (1979a) Analysis of growth of *Gluconobacter oxydans* in glucose containing media. Arch Microbiol 121:283–290

Olijve W, Kok JJ (1979b) An analysis of the growth of *Gluconobacter oxydans* in chemostat cultures. Arch Microbiol 121:291–297

Pappenberger G, Hohmann HP (2014) Industrial production of L-ascorbic acid (vitamin C) and D-isoascorbic acid. Adv Biochem Eng Biotechnol 143:143–188

Park C, Moon JY, Cokic P, Webster DA (1996) Na^+-translocating cytochrome *bo* terminal oxidase from *Vitreoscilla*: some parameters of its Na^+ pumping and orientation in synthetic vesicles. Biochemistry 35:11895–11900

Peters B, Junker A, Brauer K, Mühlthaler B, Kostner D, Mientus M, Liebl W, Ehrenreich A (2013) Deletion of pyruvate decarboxylase by a new method for efficient markerless gene deletions in *Gluconobacter oxydans*. Appl Microbiol Biotechnol 97:2521–2530

Prust C, Hoffmeister M, Liesegang H, Wiezer A, Fricke WF, Ehrenreich A, Gottschalk G, Deppenmeier U (2005) Complete genome sequence of the acetic acid bacterium *Gluconobacter oxydans*. Nat Biotechnol 23:195–200

Puustinen A, Finel M, Virkki M, Wikström M (1989) Cytochrome *o* (*bo*) is a proton pump in *Paracoccus denitrificans* and *Escherichia coli*. FEBS Lett 249:163–167

Puustinen A, Finel M, Haltia T, Gennis RB, Wikström M (1991) Properties of the two terminal oxidases of *Escherichia coli*. Biochemistry 30:3936–3942

Raspor PP, Goranovič D (2008) Biotechnological applications of acetic acid bacteria. Crit Rev Biotechnol 28:101–124

Rauch B, Pahlke J, Schweiger P, Deppenmeier U (2010) Characterization of enzymes involved in the central metabolism of *Gluconobacter oxydans*. Appl Microbiol Biotechnol 88:711–718

Richhardt J, Bringer S, Bott M (2012) Mutational analysis of the pentose phosphate and Entner–Doudoroff pathways in *Gluconobacter oxydans* reveals improved growth of a Δ*edd* Δ*eda* mutant on mannitol. Appl Environ Microbiol 78:6975–6986

Richhardt J, Bringer S, Bott M (2013a) Role of the pentose phosphate pathway and the Entner–Doudoroff pathway in glucose metabolism of *Gluconobacter oxydans* 621H. Appl Microbiol Biotechnol 97:4315–4323

Richhardt J, Luchterhand B, Bringer S, Büchs J, Bott M (2013b) Evidence for a key role of cytochrome bo_3 oxidase in respiratory energy metabolism of *Gluconobacter oxydans*. J Bacteriol 195:4210–4220

Saichana N, Matsushita K, Adachi O, Frebort I, Frebortova J (2015) Acetic acid bacteria: a group of bacteria with versatile biotechnological applications. Biotechnol Adv 33(6 pt 2):1260–1271. doi:10.1016/j.biotechadv.2014.12.001

Sakurai K, Arai H, Ishii M, Igarashi Y (2011) Transcriptome response to different carbon sources in *Acetobacter aceti*. Microbiology 157:899–910

Sakurai K, Arai H, Ishii M, Igarashi Y (2012) Changes in the gene expression profile of *Acetobacter aceti* during growth on ethanol. J Biosci Bioeng 113:343–348

Sarkar D, Yabusaki M, Hasebe Y, Ho PY, Kohmoto S, Kaga T, Shimizu K (2010) Fermentation and metabolic characteristics of *Gluconacetobacter oboediens* for different carbon sources. Appl Microbiol Biotechnol 87:127–136

Schweiger P, Gross H, Zeiser J, Deppenmeier U (2013) Asymmetric reduction of diketones by two *Gluconobacter oxydans* oxidoreductases. Appl Microbiol Biotechnol 97:3475–3484

Shinjoh M, Setoguchi Y, Hoshino T (1990) Sorbose dissimilation in 2-keto-L-gulonic acid-producing mutant UV10 derived from *Gluconobacter melanogenus* IFO 3293. Agric Biol Chem 54:2257–2263

Sootsuwan K, Lertwattanasakul N, Thanonkeo P, Matsushita K, Yamada M (2008) Analysis of the respiratory chain in ethanologenic *Zymomonas mobilis* with a cyanide-resistant *bd*-type ubiquinol oxidase as the only terminal oxidase and its possible physiological roles. J Mol Microbiol Biotechnol 14:163–175

Sugiyama M, Suzuki S, Tonouchi N, Yokozeki K (2003) Transaldolase/glucose-6-phosphate isomerase bifunctional enzyme and ribulokinase as factors to increase xylitol production from D-arabitol in *Gluconobacter oxydans*. Biosci Biotechnol Biochem 67:2524–2532

Tonouchi N, Sugiyama M, Yokozeki K (2003) Coenzyme specificity of enzymes in the oxidative pentose phosphate pathway of *Gluconobacter oxydans*. Biosci Biotechnol Biochem 67:2648–2651

van der Oost J, Schepper M, Stouthamer AH, Westerhoff HV, van Spanning RJ, de Gier JW (1995) Reversed electron transfer through the bc_1 complex enables a cytochrome *c* oxidase mutant (Δaa_3/cbb_3) of *Paracoccus denitrificans* to grow on methylamine. FEBS Lett 371:267–270

Yakushi T, Matsushita K (2010) Alcohol dehydrogenase of acetic acid bacteria: structure, mode of action, and applications in biotechnology. Appl Microbiol Biotechnol 86:1257–1265

Zhang P, Ma Y, Wang F, Wei D (2014) Phosphorylation of HPr by HPr kinase in *Gluconobacter oxydans* 621H. Protein Pept Lett 21:597–601

Zhong C, Zhang GC, Liu M, Zheng XT, Han PP, Jia SR (2013) Metabolic flux analysis of *Gluconacetobacter xylinus* for bacterial cellulose production. Appl Microbiol Biotechnol 97:6189–6199